High Frequency Switching Power Converter for Ultrasonic Welding Application

A Thesis

Submitted by

Mohit Mangal

in partial fulfilment of the requirement for the award

of the degree of

MASTER OF TECHNOLOGY

DEPARTMENT OF ELECTRICAL ENGINEERING

INDIAN INSTITUTE OF TECHNOLOGY MADRAS

CHENNAI-600 036, INDIA

JUNE 2021

Thesis Certificate

This is to certify that the thesis entitled **"High Frequency Switching Power Converter for Ultrasonic Welding Application"** submitted by **Mohit Mangal (EE19M039)** to the Indian Institute of Technology, Madras for the award of the degree of **Master of Technology** is a bona fide record of research work carried out by him under my supervision. The contents of this thesis, in full or in parts, have not been submitted to any other Institute or University for the award of any degree or diploma.

Dr. N.Lakshminarasamma

Associate Professor

Dept. of Electrical Engineering

IIT-Madras, 600 036

Place: Chennai

Date: June 2021

Acknowledgment

I would like to express my sincerest gratitude to Dr. N.Lakshminarasamma for giving me the opportunity to work on a project as ambitious as this one. The experiences I have gathered and the invaluable lessons I have learned while working on this project have endowed me with a renewed interest in the area of resonant converters and ultrasonic transducer and this would not have been possible without her guiding me every step of the way. I would like to thank my Power electronics group members Nagesha and Vivek for guiding me on this project. I would like to thank my parents for always supporting me no matter what. It is their support that gave me the assurance needed to pursue an M.Tech instead of doing a job.

Abstract

Ultrasonic welding is the process of bonding elements using ultrasonic acoustic vibrations delivered locally to bonded elements held together under pressure. It is most commonly used for joining plastic elements, but it can also be used to join thin metal foils and non-woven fabrics. Ultrasonic technology utilizing similar devices as ultrasonic welding can also be used to process liquids, i.e. mixing paints, or purifying waste water.

The purpose of this thesis is to investigate the technology of designing the power supply and control for ultrasonic welding machine. The proposed converter uses LLCC resonant converter for the ultrasonic welding generator. Phase shift control is proposed for the precise power control of ultrasonic welding generator. Envelope modeling provides a simple and easy method to get the small signal transfer function model. Simulations were carried out for Ultrasonic welding generator in MATLAB software. Closed loop control is done in PLECS software.

Contents

List of Figures

List of Tables

Chapter 1

Introduction

1.1 Ultrasonic Welding

Ultrasonic welding is based on the introduction of a certain type of acoustic waves to the welded material. This process is also used in ultrasonic drilling, cutting and cleaning. Typical frequency range used is between 18 kHz and 70 kHz. Output power varies from hundreds W to a few kW. Standard welding system consists of an electrical power supply (generator), and ultrasonic stack consisting of a transducer, booster and sonotrode (horn). The generator is responsible for supplying correct electrical signal to the transducer as well as for process control. Transducer transforms electrical supply signal into mechanical longitudinal vibrations which are transferred to sonotrode and ultimately to the welded material [1]. An example of ultrasonic welding machine is shown in [Figure 1.1].

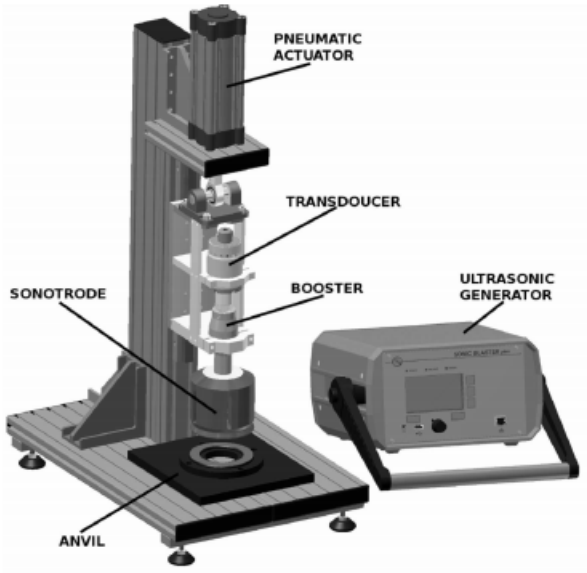

Figure 1.1: Simplified model of an Ultrasonic Welding Machine

1.2 Basic Elements of Ultrasonic Welding Machine

The basic elements of ultrasonic welding machine are press, ultrasonic stack , converter , booster , sonotrode . The basic elements are described in detail in this section below :

Press: A press is needed to put the parts to be assembled under pressure to weld or to cut. It is usually automated by using PLC. A nest or anvil where the parts are placed and allowing the high frequency vibration to be directed to the interfaces.

Ultrasonic Stack: An ultrasonic stack composed of a converter or piezoelectric transducer, an optional booster and a sonotrode (US: Horn). All three elements of the stack are specifically tuned to resonate at the same exact ultrasonic frequency (Typically 20, 30, 35 or 40 kHz).

Converter: Converts the electrical signal into a mechanical vibration.

Booster: Modifies the amplitude of the vibration. It is also used in standard systems to clamp the stack in the press.

Sonotrode: Applies the mechanical vibration to the parts to be welded.

From the electrical point of view, the ultrasonic stack can be represented as equivalent RLC circuit (commonly known from literature as Butterworth van-Dyke model) shown in [Figure 1.2]. This model allows for complex electrical simulation of generator - ultrasonic stack system. C, L and R elements represent the mechanical properties of the stack, while Co represents parallel capacitance of the piezoceramic disks [2]. Ultrasonic stack is typically supplied with a sinusoidal waveform with a voltage of 1 kV to 2 kV RMS, and frequency selected from 20 kHz to 70 kHz (20 kHz systems are the most commonly used). The ultrasonic stack bandwidth is usually very narrow, which requires the generator to precisely monitor and tune itself to the resonance point of the stack. The accuracy of this tuning is often required to be better than 1 Hz at 20 kHz output frequency.

Ultrasonic Generator: An electronic ultrasonic generator delivering a high power (2 kW - 3 kW) AC signal with frequency matching the resonance frequency of the stack.

1.3 Process

During the ultrasonic welding or cutting process the welded or cut elements are placed between the steel anvil and sonotrode and are pressed together with the pneumatic actuator at the pressure of up to 1 MPa. Then the ultrasonic welding or cutting cycle is started,

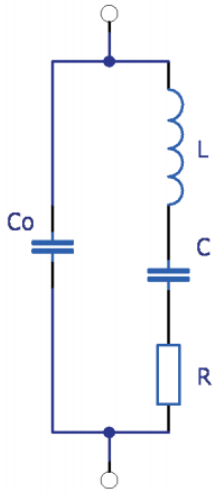

Figure 1.2: The electrical equivalent circuit of the ultrasonic assembly

i.e., the ultrasonic power supply starts to generate an electric signal feeding the ultrasonic stack consisting of the high power ultrasonic electro-mechanic transducer, the booster, and the sonotrode. The mechanical vibrations generated by the transducer are amplified by the booster and sonotrode assembly. As the result, the mechanical vibrations amplitude at the sonotrode working surface can be as high as tens of micrometers. The mechanical waves propagate through the welded elements causing the melting and mixing of particles of the welded materials forming a firm joint. The ultrasonic welding and cutting process is very fast and energy efficient, because the ultrasonic energy is supplied exactly where it is needed and in short bursts. Moreover, there is no need to use additional substances such as glues, solvents, rivets. The resulting joint is uniform, clean, tight, and of high strength – often higher than the strength of welded elements. Thanks to these advantages, the ultrasonic welding and cutting technology has been widely used recently, and it gradually replaces all

other traditional bonding technologies. Ultrasonic welding has great advantages over other joining techniques. It is a very fast process. A single joint can be created in under 1 second. However, to develop a good – i.e., efficient, reliable, and producing high quality joints – ultrasonic welding and cutting system, a couple of key development problems must be taken into account and solved. In fact, the contemporary ultrasonic welding and cutting system is a product of mechatronics , where mechanics, electronics, informatics, and control must be combined in order to obtain usable and high quality products. In this report, the most vital element of an ultrasonic welding and cutting system – i.e., the ultrasonic power supply – has been under consideration.

Precise stabilization of the ultrasonic power during the process is essential to maintain high reliability and repeatability of the welds. This is especially important in processing fragile materials, as well as welding small plastic elements and in continuous welding with rotating sonotrode. During the welding process melting and compression of the welded material causes variations in power transfer ratio to the material. In ultrasonic drilling and cutting erosion of the material also causes such variations. Those variations have negative impact on the quality of processed elements. It results in inconsistent weld where some part of the material is damaged by excessive power and some part is welded weakly or not welded at all. To prevent such situations welding system must constantly monitor power delivery level and assure it remains constant [1].

1.4 Ultrasonic Generator

The main task of the generator is to transmit power to the transducer in such a way that the transducer is most efficient at transforming electrical power into mechanical vibration power. Output waveform of ultrasonic generator is sinusoidal and output frequency of particular generator is variable in narrow range. Narrow frequency band and sinusoidal output voltage allow the use of a resonant converter. Such a solution eliminates commutation losses in power switching transistor, hence has better efficiency compared to other converter designs. This approach was used to design ultrasonic generator presented in this report. The unit can deliver to the load up to 3 kW of continuous power in 20 kHz version.

The Ultrasonic Generator has the greatest impact on the performance and reliability of the ultrasonic welding system. Temperature and load have a significant influence on the ultrasonic stack parameters. During the welding process, the generator is forced to constantly monitor stack parameters, and change output frequency and voltage accordingly. Digital measurements of output voltage and current, and digital signal processing algorithms can greatly increase the stability of generator control loop. Cycle by cycle parameters monitoring can also protect both the generator and ultrasonic stack from overload and damage.

Chapter 2

Power Converter

2.1 Ultrasonic Transducer

The ability of a piezoelectric transducer in energy conversion is rapidly expanding in several applications. Some of the industrial applications for which a high power ultrasound transducer can be used are surface cleaning, water treatment, plastic welding and food sterilization. Also, a high power ultrasound transducer plays a great role in biomedical applications such as diagnostic and therapeutic applications. An ultrasound transducer is usually applied to convert electrical energy to mechanical energy and vice versa. In some high power ultrasound system, ultrasound transducers are applied as a transmitter, as a receiver or both. As a transmitter, it converts electrical energy to mechanical energy while a receiver converts mechanical energy to electrical energy as a sensor for control system. Once a piezoelectric transducer is excited by electrical signal, piezoelectric material starts to vibrate and generates ultrasound waves. To drive an ultrasound transducer, an excitation

signal should be properly designed otherwise undesired signal (low quality) can deteriorate the performance of the transducer (energy conversion) and increase power consumption in the system.

2.1.1 Piezoelectric Converter Model

There are many possibilities to present and analyze equivalent models of piezoelectric converters. Modeling can be done for High-power piezoelectric, Langevin, sandwich-converters (applicable in ultrasonic cleaning, plastic welding, sonochemistry and other power industrial applications). For electrical engineering needs (as for instance: when optimizing ultrasonic power supplies, in order to deliver maximal ultrasonic power to a mechanical load) we need sufficiently simple and practical (lumped parameter), equivalent models, expressed only using electrical (and easy measurable or quantifiable) parameters (like resistance, capacitances, inductances, voltages and currents). Of course, in such models we should (at least) qualitatively know which particular components are representing purely electrical nature of the converter, and which components are representing mechanical or acoustical nature of the converter, as well as to know how to represent mechanical load.

The best lumped parameter equivalent circuits that are fitting a typical piezoelectric-converter impedance (the couple of series and parallel resonance of an isolated vibration mode) are shown to be Butterworth-Van Dyke (BVD) and/or its electrical dual-circuit developed by Redwood (booth of them derived by simplifying the Mason equivalent circuit and/or making the best piezoelectric impedance modeling based on experimental results

and electromechanical analogies).

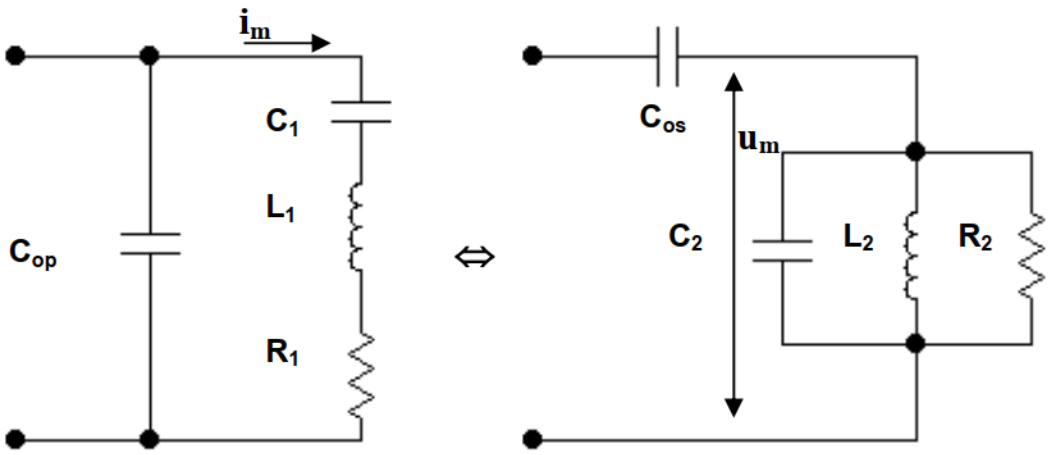

Figure 2.1: Butterworth-Van Dyke, dual-circuits models

The [Figure 2.1] presents two of the most widely used lumped-parameters piezoelectric converter impedance models (mutually equivalent, BVD = Butterworth-Van Dyke, dual-circuits models), valid for isolated couple of series and parallel resonances (of a non-loaded). In fact, on the [Figure 2.1] are presented the simplest models applicable for relatively high mechanical quality factor piezoelectric converters, where thermal dissipative elements in piezoceramics could be neglected.

In the above given converter model, we can recognize motional current i_m and motional voltage u_m as the most important mechanical-output power/amplitude controlling parameters of piezoelectric converters in series and parallel resonance. When converter is operating in series resonance, in order to control its output power and/or amplitude we should control its motional current i_m, and in the regime of parallel resonance, output power and/or ampli-

tude are directly proportional to the motional voltage u_m. More precisely, when we compare two operating regimes of the same converter, when converter is producing the same output power (in series and/or parallel resonance), we can say that converter operating in series resonance is able to deliver to its load high output force (or high pressure) and relatively low velocity, and when operating in parallel resonance it is able to deliver high output velocity and relatively low force (knowing that output converter power is the product between velocity and force delivered on its front emitting surface).

Here we are using the electromechanical analogy system: $(Current \leftrightarrow Force)$ & $(Voltage \leftrightarrow Velocity)$. When we are talking about converter's series-resonance frequency zone, this is the case of motional Current- Force resonance (where converter's impedance has low values), and when we are talking about converter's parallel-resonance frequency zone, this is the case of motional Voltage-Velocity resonance (where converter has high impedance values). Automatically, if we realize by electrical means high motional current (current resonance, equal to series resonance), the converter will produce high motional force (it will operate in a force resonance). Also, if we realize by electrical means high motional voltage (voltage resonance, equal to parallel resonance), the converter will produce high motional velocity [2] (it will operate in a velocity resonance). All above conclusions, for the time being, are based only on the analogy $(Current \leftrightarrow Force)$ & $(Voltage \leftrightarrow Velocity)$.

2.1.2 Ultrasonic Transducer Impedance characteristics

The critical behaviour of a piezoelectric device is encapsulated in its resonant frequencies, and the most efficient way to find the critical piezoelectric specifications is by studying its impedance frequency response. [Figure 2.2] illustrates a sample piezoelectric impedance as a function of frequency. As the figure shows, piezoelectric devices typically have two kinds of electrical resonances, the first one known as resonant frequency (fr) and the other one known as anti-resonant frequency (fa). A knowledge of such impedance characteristics is important for electrical circuit modelling of the piezoelectric devices. In the case of high power applications, knowledge of the impedance characteristics is important so that maximum transmission performance can be achieved.In the other words, at resonant frequencies, piezoelectric elements convert the input electrical energy into mechanical energy most efficiently, and so it is necessary to accurately extract these frequencies and excite the system appropriately. Piezoelectric devices typically have multiple resonant frequencies but only the major resonant frequency is generally targeted for excitation in practice [4].

$$fs = \frac{1}{2\pi\sqrt{L_1 C_1}}$$

$$fp = \frac{1}{2\pi\sqrt{L_1 C_1 C_{op}/(C_1 + C_{op})}}$$

Universal ultrasonic generator must be able to adapt to changes of ultrasonic stack parameters. The device must be able to perform diagnostics of the stack. In the first step the generator has to measure the electrical impedance of the stack as a function of frequency in the frequency range covering operational range of the generator type. For instance, generator designed for 20 kHz technology should operate in the range of 19 kHz up to 21 kHz. Example

of such measurement is shown in [Figure 2.2]. The second step is the estimation of the series resonance frequency and parallel resonance frequency of the stack. Those parameters are essential for proper operation of the generator and are used in the process of output power control.

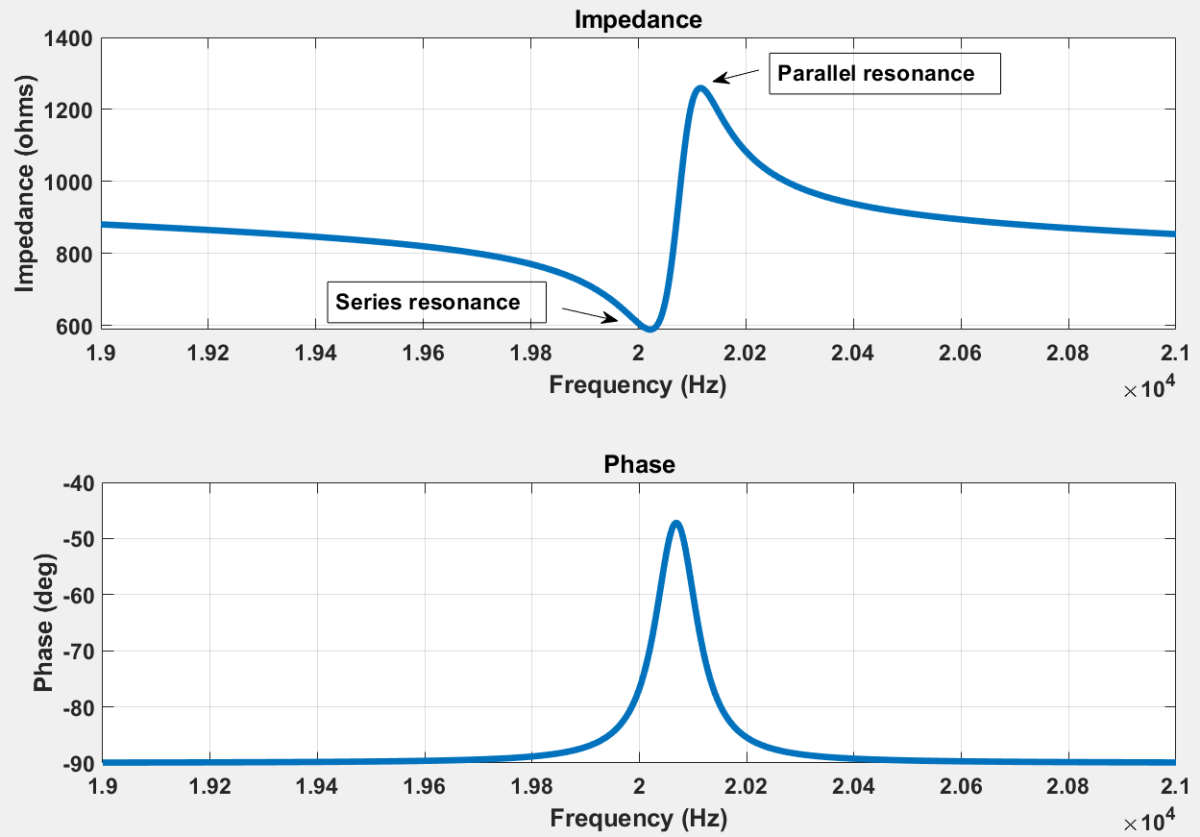

Figure 2.2: Impedance-Phase Characteristics

2.1.3 Inductive Compensation

Series inductive compensation is naturally enabling converter to produce real (active) power in its parallel mechanical-resonance fp, and parallel inductive compensation is naturally enabling converter to produce real power in its series mechanical-resonance fs. One of the problems for designers in this field is that both, series and parallel inductive compensations are creating two more side-band resonant zones.

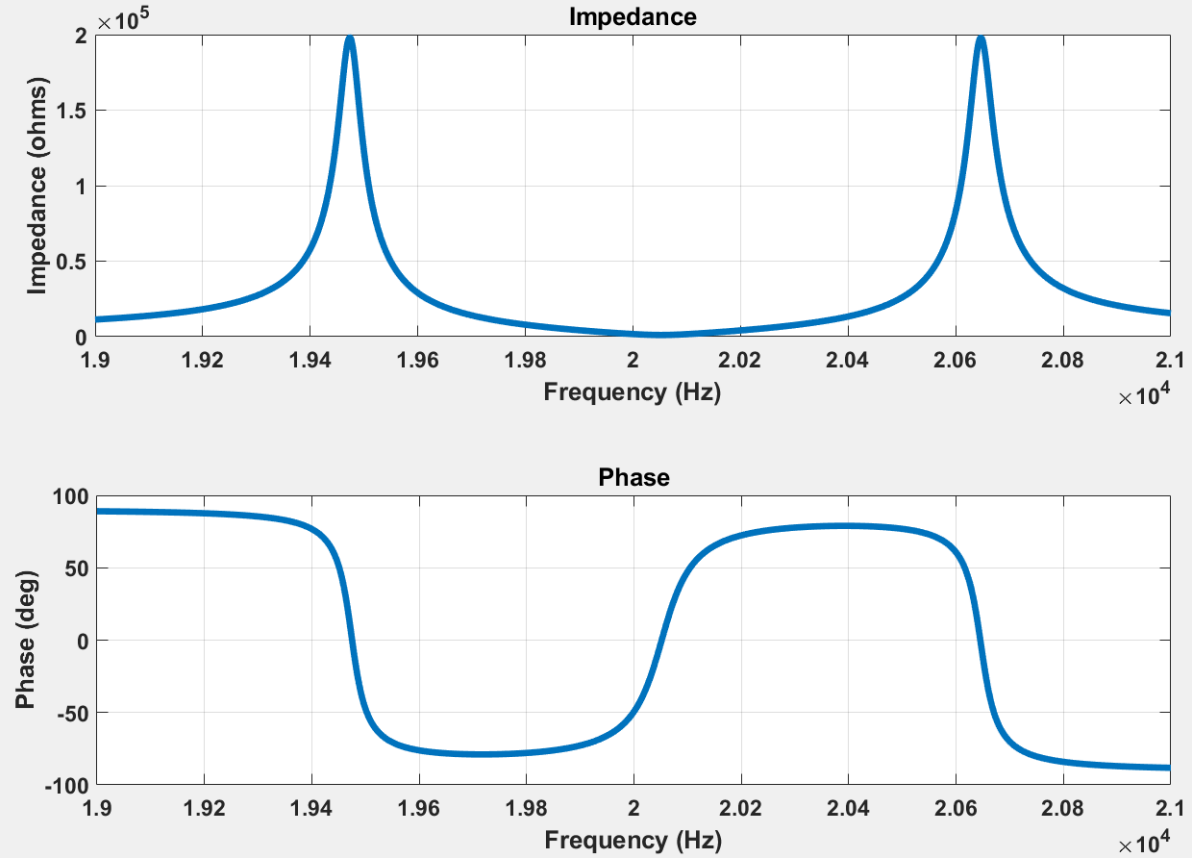

Figure 2.3: Impedance-Phase Characteristics with Inductive Compensation

The purpose of making inductive compensation of piezoelectric converters is not only

to enable them operating efficiently on a stable (constant) resonant frequency. Applying proper inductive compensation (or combined parallel and series inductive compensation) we can also make converter operating efficiently in a relatively large frequency interval (for instance in the interval between series and parallel resonant frequency), maximize active (or real) output converter-power, and control particular mechanical output/s such as: output oscillatory speed, acceleration and amplitude.

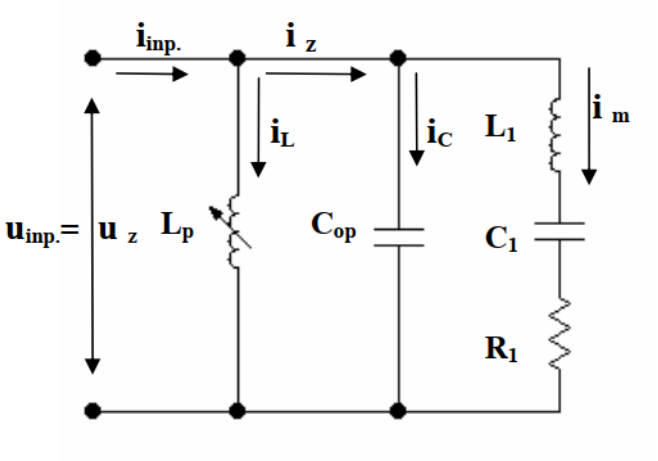

Figure 2.4: Ultrasonic Transducer with Parallel Inductive Compensation

$$Lp = \frac{1}{4\pi^2 f_s^2 C_{op}}$$

Now, we can analyze interesting aspects of parallel inductive compensation, when converter operates in its series mechanical resonance fs. The input driving-signal in this case is input current I_{in} and mechanical output is represented by motional current i_m, effectively representing converter's output force . The objective of optimal power and frequency control (and best inductive matching) in this case is to realize linear dependence between I_{in} and i_m , or to make them mutually equal and in phase in the largest possible frequency interval

while having series mechanical resonance fs in the middle point of that interval (fs $\approx 0.5(f_{PH}$ + f_{PL})). This way, by controlling the input current we are effectively controlling the output force. Of course, in order to control the input current I_{in}, we need to detect converter motional current i_m and to use it as the feedback information for automatic, closed-loop regulation[2].

2.2 Resonant converter

From the features of the converter presented in the previous section of ultrasonic and the vibrating system it follows that the generator intended to work in the welding system must meet the following assumptions:

- provide compensation of the converter's own capacitance to minimize the converter reactive power.
- provide high voltage sinusoidal wave with sufficient current capacity.
- allow waveform frequency adjustment in narrow frequency range with very high resolution.
- generator should be highly efficient and reliable.

Output waveform of ultrasonic generator is sinusoidal and output frequency of particular generator is variable in narrow range. Narrow frequency band and sinusoidal output voltage allow the use of a resonant converter.Such a solution eliminates commutation losses in power switching transistor, hence has better efficiency compared to other converter designs[3].

2.2.1 Generator Power stage

Generator Power stage consists of:

- Full bridge MOSFET Switching circuit
- Resonant tank
- Transformer
- Parallel Inductive compensation

Figure 2.5 presents a simplified electrical schematic of the resonant converter used in the design. It consists of a Full bridge MOSFET switching circuit which generates square signal with variable duty cycle. When the generator is in the first stage of the power control algorithm, in which output voltage is being changed, the duty cycle is between 0% and 50% .Signal from the switching circuit is fed to a series resonance circuit. The circuit forms sinusoidal signal transferred to the power transformer which rises output voltage to appropriate level. Q factor of the LC tank is selected in such a way as to provide the ability to tune generator output frequency to the resonance frequency of the ultrasonic stack, and at the same time provide low distortion levels in the output signal. There is an additional inductance in the output stage of the generator which is used to compensate the parallel capacitance of the transducer. The compensating inductance and the transducer internal parallel capacitance form a parallel resonance circuit. This circuit has also low Q-factor and resonance frequency equal to the middle of the generator frequency range[1].

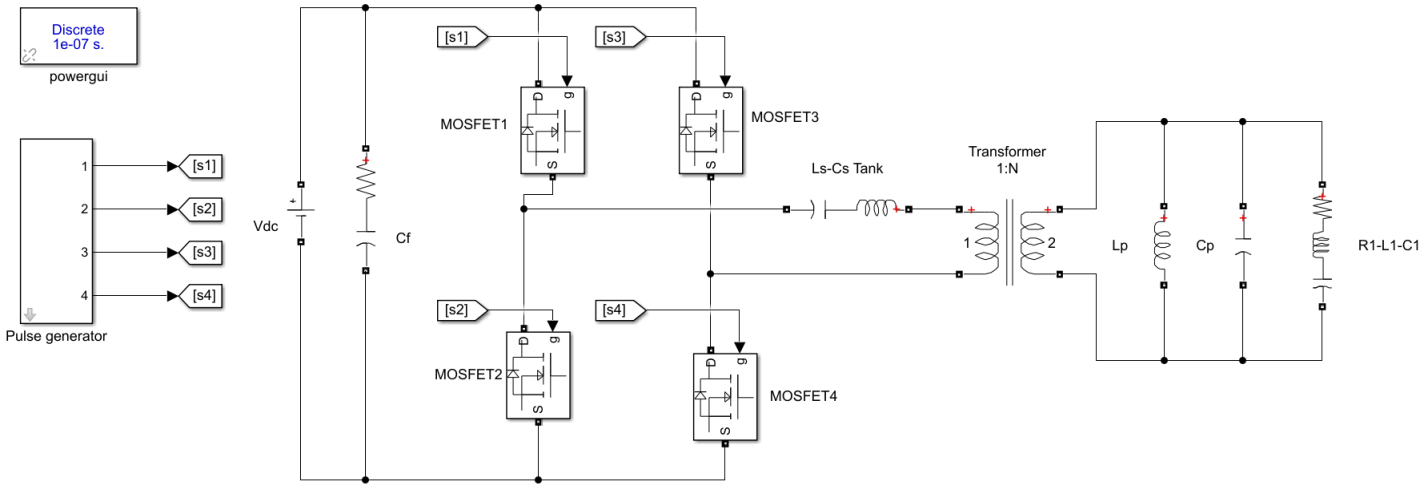

Figure 2.5: Matlab simulink model for Ultrasonic Generator

Chapter 3

Design and Simulation

Of central importance in design of a resonant converter is the selection of the resonant tank topology and element values, so that the transistor conduction losses at light load are minimized, so that zero-voltage switching is obtained over a wide range of load currents (preferably, for all anticipated loads, but at least at full and intermediate load powers), and so that the converter dynamic range is compatible with the load i–v characteristic.

Frequency domain analysis techniques, and variants thereof, are often preferred tools when the protracted simulation times associated with traditional circuit simulators are considered too lengthy. When designing a resonant converter with a high-load quality factor (Q), higher harmonics of the input can be considered to be sufficiently filtered so they present a negligible contribution to the output, thereby allowing equivalent sinusoidal voltage and current sources to appear at the input to the tank, and permit the use of Fundamental Mode Approximation (FMA) to be employed to predict the steady state behaviour of the converter[5].

3.1 Design Consideration

The LLCC-resonant inverter consists a series-resonant circuit consisting of capacitor Cs and inductor Ls and a parallel resonant circuit consisting of inductor Lp and equivalent piezoelectric capacitor Cp. Note that besides the higher part count, the circuit can make use of the parasitics of the transformer: Part of Ls is contributed by the leakage inductance of the transformer, while Lp can be donated by a wider air-gap of the transformer.

Then the impedance of the LLCC-resonant circuit is

$$Z_{LLCC}(jw) = jwL_s + \frac{1}{jwC_s} + \frac{1/n^2}{\frac{1}{jwL_p} + jwC_p + \frac{1}{Z_1(jw)}}$$

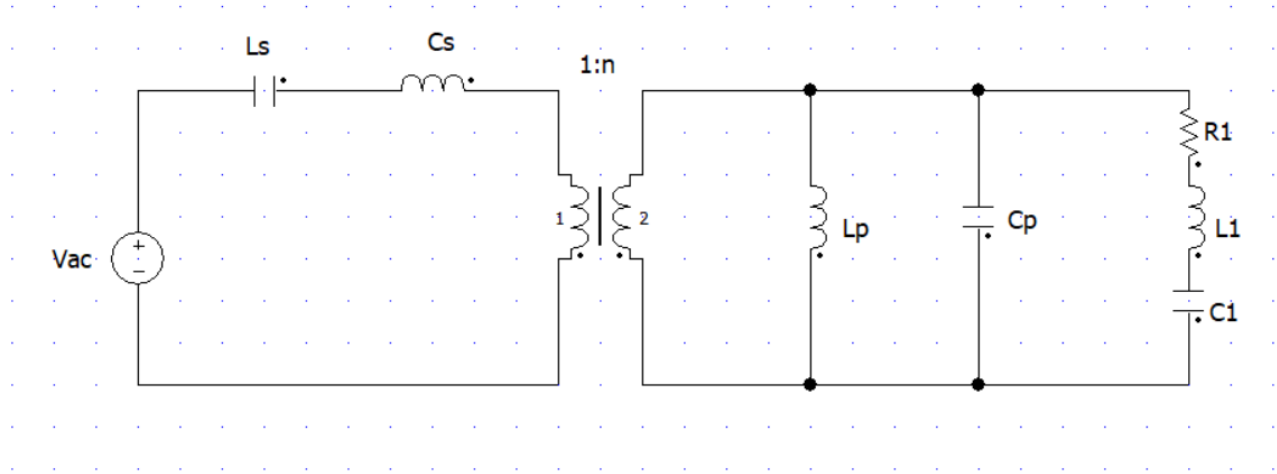

Figure 3.1: LLCC Resonant Converter

where Z_1(jw) is the equivalent impedance of the piezoelectric Transducer, which represents a mechanical resonant part.

$$Z_1(jw) = jwL_1 + \frac{1}{jwC_1} + R_1$$

If the driving frequency of the piezoelectric actuator is the same as the mechanical resonance frequency, the $L_1 - C_1 - R_1$ circuit behaves as a purely resistive load R_1. For easy calculation we are using 1:1 ratio for transformer.

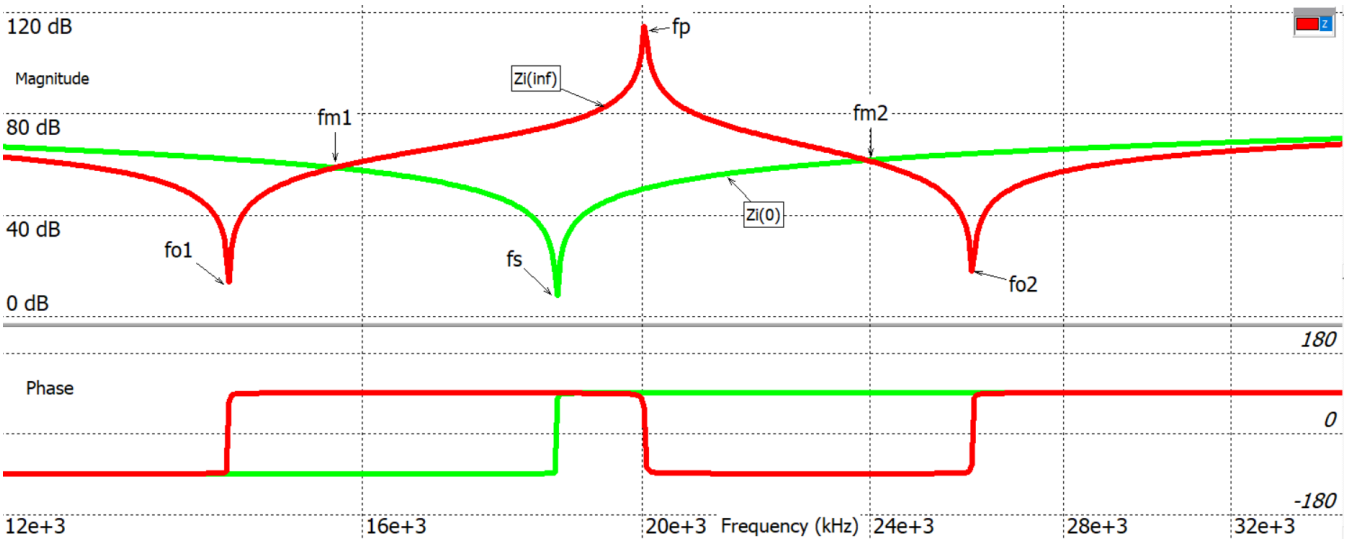

Figure 3.2: Input impedances of converter

In the above [figure 3.2], magnitude and phase of Zi(0) is found with load R_1 shorted and for Zi(inf) is found with load R_1 open-circuited . The resonant frequency of the parallel resonance network Lp-Cp is

$$w_p = \frac{1}{\sqrt{LpCp}}$$

The resonant frequency of the series resonance network Ls-Cs is

$$w_s = \frac{1}{\sqrt{LsCs}}$$

The effective resonant frequency of the complete tank are

$$w_{o1} = w_s \sqrt{\frac{1 + Ln + Cn - \sqrt{(1 + Ln + Cn)^2 - 4LnCn}}{2Cn}}$$

$$w_{o2} = w_s \sqrt{\frac{1 + Ln + Cn + \sqrt{(1 + Ln + Cn)^2 - 4LnCn}}{2Cn}}$$

where

Ln = Ls/Lp

Cn = Cp/Cs

It should be noted,that four reactive components exist in this converter topology, it is their ratios that are important from a design perspective[5]. For initial design we are taking both the ratios to be equal.

$$Ln = Cn = \alpha$$

Increasing α, the first resonance frequency w_{o1} is increased and the second w_{o2} is decreased, without changing the operating frequency of the piezoelectric actuator f_p. If a smaller α is used, the required Ls becomes smaller, and at the same time a larger Cs has to be employed. When α decreases, the voltage gain G of the converter is also increased at the frequency $w \geq w_{o2}$, then the suppression of harmonic components of inverter output voltage will be decreased. Specially stronger influence takes place at the 3rd, 5th, 7th and 9th harmonic components, which dominate the harmonics of inverter voltage [7].

Transducer Parameters	Value
C_{op}	9.2 nF
R_1	1100 ohm
L_1	2 H
C_1	31.5 pF

Table 3.1: Transducer Parameters used for simulation

3.2 Required Specifications

For designing a 3 kW ultrasonic Welding Generator at 20 kHz switching frequency we have taken Ultrasonic Transducer parameters as shown in table 3.1. Input DC voltage is taken as 350 V for the purpose of Simulation. The requirement is to have Sinusoidal Voltage at the output with a 20 kHz frequency having magnitude(rms) of around 1.9 kV. As the required power level is high, we have used a Full bridge switching converter with four Mosfet switches[3].

3.3 Design of Tank Parameters

We know the parameters from the previous section, the series resonant frequency and the parallel resonant frequency can be found. Once we know the value of series resonant frequency, we can find the value of parallel inductance for the reactive power compensation. The calculated values are shown in table 3.3.

Now, designing of the series Resonant tank parameters can be done by selecting the

Parameters	Value
Resonant Frequency	20051.64 Hz
Anti resonant frequency	20085.94 Hz
L_p	6.848 mH

Table 3.2: Calculated Values Transformer secondary side

proper value of Ls and Cs according to the requirements. Primary LC tank, composed of Ls and Cs elements, is responsible for forming a sinusoidal waveform delivered to the transformer. Q factor of the LC tank is selected in such a way as to provide the ability to tune generator output frequency to the resonance frequency of the ultrasonic stack, and at the same time provide low distortion levels in the output signal. Transformer increases output voltage to nominal 1.9 kV RMS at full power.Output compensating coil, L_p, is added to provide apparent power compensation of ultrasonic transducer parallel capacitance C_{op}. Selection of compensating coil value is done for particular types of ultrasonic transducer.

As seen from the [figure 3.2] it can be observed that, when the switching frequency is $fs < f < fp$, ZVS can be achieved for all loads. When the switching frequency is $f < fo1$,ZCS can be achieved for all loads.when the switching frequency is $f > fo2$, ZVS can be achieved for all loads. Zi(inf) is greater than Zio between $fm1 < f < fm2$.

For the frequency range $fp < f < fm2$,we can observe that for heavy load ZVS is happening and for light loads ZCS is happening. So in this range we can say that for $R < R_{critical}$, we will get Zero voltage switching [6].

For initial design We are taking $Ln = 3$, $Cn = 3/1.15$ and $n = 6.37$. Based on these design

Parameters	Value
C_p	9.2 nF
L_p	6.848 mH
L_s	506.3 uH
C_s	0.143 uF
n	6.37

Table 3.3: Calculated Values Transformer secondary side

value we are able to get less than 5% THD in output voltage and less than 1% THD in output current i_m.

3.4 Simulation Results

All the simulation work for this project has been done in MATLAB Simulink software. With the use of LLCC topology we are able to get almost constant voltage gain for a required operating range of frequency. Some of the important voltage and current waveforms have been shown below:

3.4.1 Voltage Waveforms

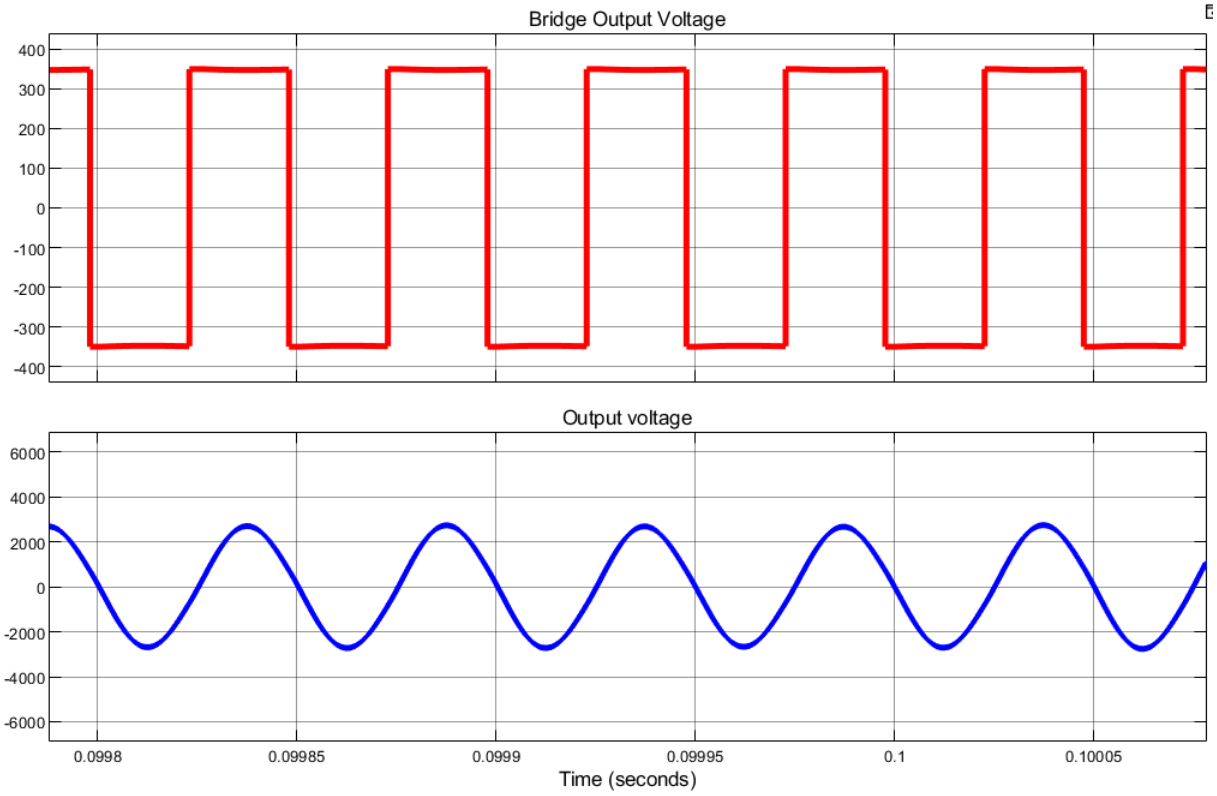

Figure 3.3: Voltage Waveforms

3.4.2 Current Waveforms

Bridge Output current, Transformer Secondary current and output current are shown in [Figure 3.4]. Tank current waveforms are shown in [Figure 3.5].

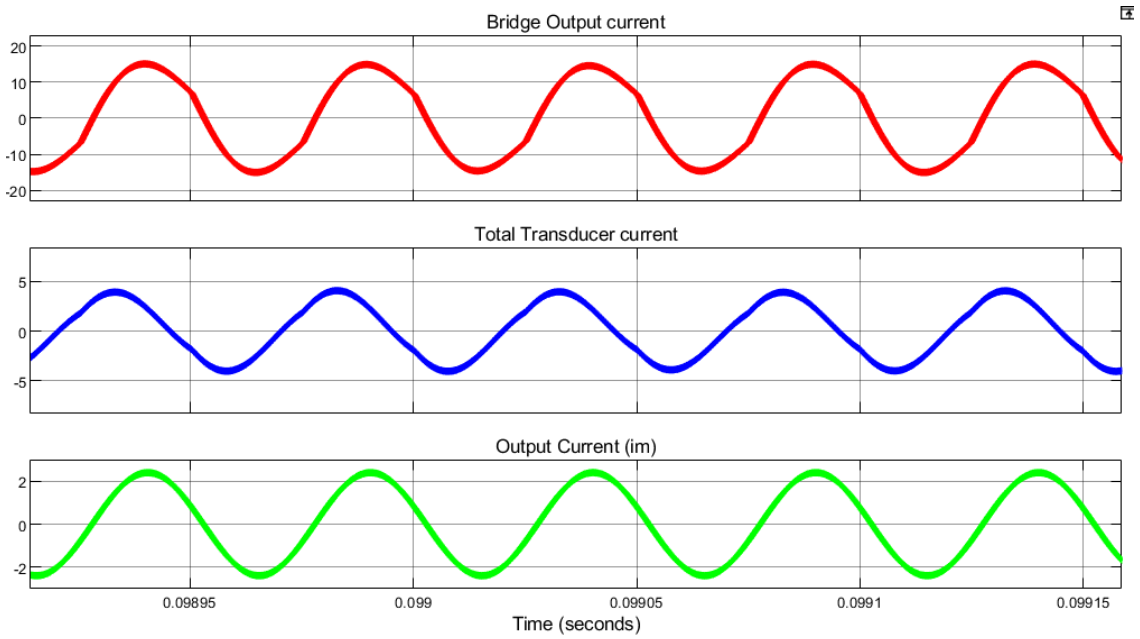

Figure 3.4: Current Waveforms

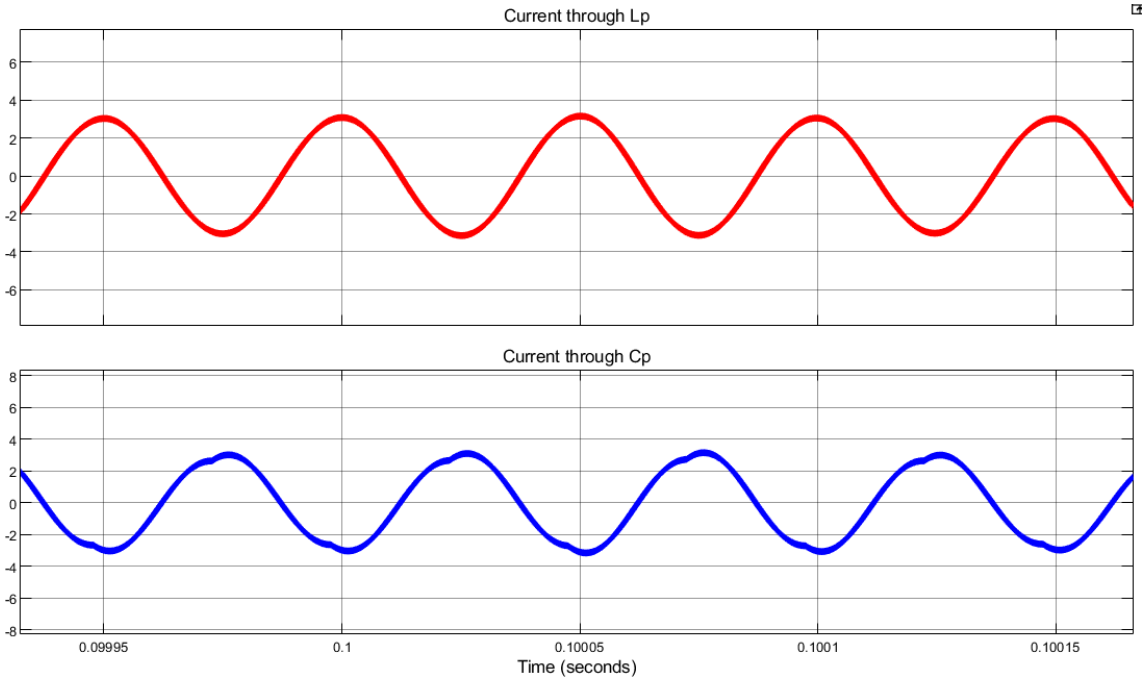

Figure 3.5: Parallel Tank Element current

3.4.3 Switching Waveforms

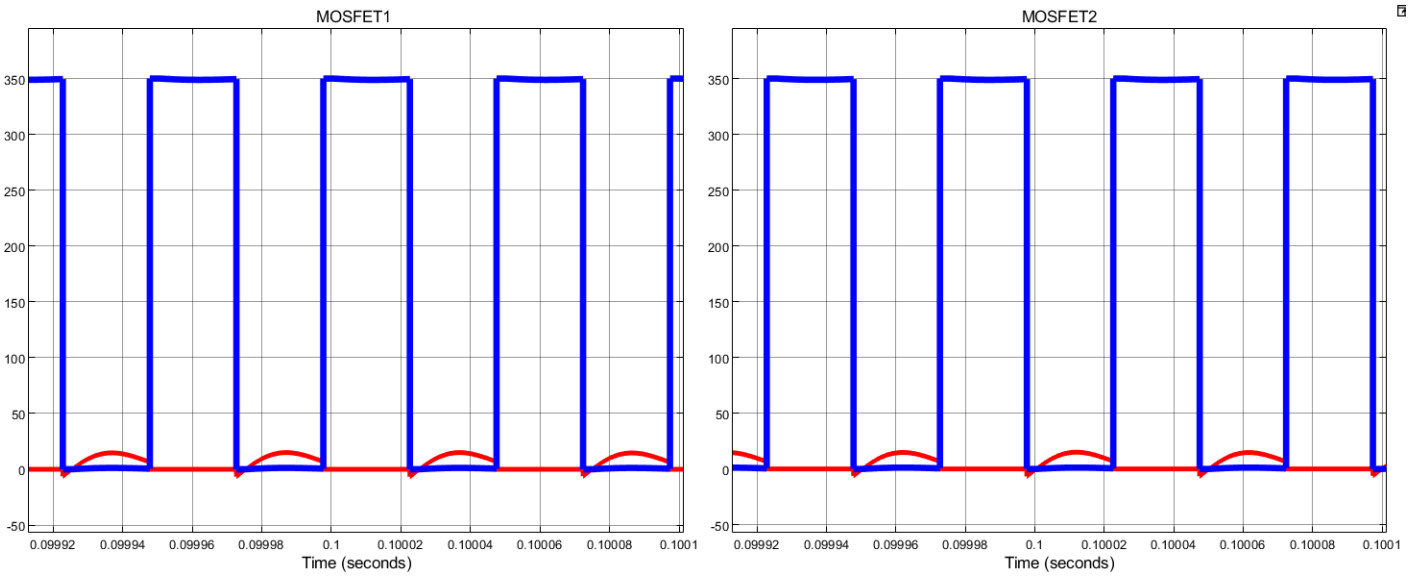

Figure 3.6: Voltage and Current waveforms of Mosfet Switches

Chapter 4

Modeling and Control of LLCC Resonant converter

High-frequency dc-to-ac inverters are used in a variety of applications. The dc power input is generally converted to a high frequency ac output through use of a switch network followed by a resonant tank . The output power can then be regulated by controlling the bus voltage and/or the switching frequency. This is due to the frequency dependant nature of the resonant tank, where input variations in both the bus voltage (amplitude modulation, AM) and the switching frequency (frequency modulation, FM) result in amplitude variations at the load. Thus the objective of the controller is to regulate the envelope or magnitude of the signals at the load. A common objective with a long history is to model the ac dynamics from input modulation to output envelops in order to facilitate optimized controller design. Several approaches are available to model the envelope dynamics of a resonant inverter.

One of the possible approach is to decompose the modulated input (AM or FM) into three dominant components: its fundamental component plus two sidebands. The overall response of the linear system to the modulated input is considered as the summation of the responses to the three individual inputs. Then the small signal transfer functions from bus voltage/switching frequency to output envelops can be obtained.

4.1 Small Signal Modeling

The spectrum of the square-wave V_s contains a fundamental ac component as well as higher-order harmonics. If the switching frequency is close to the resonant frequency fr and the tank has high Q-factor, then the higher order harmonics of $v_s(t)$ will be filtered by the resonant tank such that the load current and voltage are essentially sinusoidal with frequency f,. Hence the sinusoidal approximation can be applied, which greatly simplifies the analysis[8].

$$V_{s1} = \frac{4V_g}{\pi}\cos(w_s t)$$

Next, we introduce a small variation in the control input. In response, the frequency modulator (VCO) varies the switching frequency fs as follows:

$$f_s(t) = F_s + \hat{f}_s(t)$$

$$\hat{f}_s(t) = \Delta f \cos(w_m t)$$

$$w_s(t) = w_{s0} + \Delta w \cos(w_m t)$$

where

$$\Delta w = 2\pi\Delta f$$

$$w_{s0} = 2\pi F_s$$

Then,

$$V_{s1} = \frac{4V_g}{\pi}\cos(w_s t + \beta \sin(w_m t))$$

where modulation index β is

$$\beta = \frac{\Delta w}{w_m}$$

V_{s1} can be expanded using Bessel functions. Bessel functions are used to determine the amplitude of the carrier and the resulting sideband frequencies. Bessel functions has the advantage of determining the locations of the modulated frequencies in the frequency spectrum, as well as giving the amplitude of each frequency component . Assuming narrow band frequency modulation i.e. the value of modulation index $\beta << 1$, higher order sidebands can be neglected[8].

$$V_{s1} \approx \frac{4V_g}{\pi}\cos(w_{s0}t) + \frac{\beta}{2}\cos((w_{s0} + w_m)t) - \frac{\beta}{2}\cos((w_{s0} - w_m)t)$$

The tank transfer function H(s) operates on each of these frequency components, and we can compute the resulting output voltage v(t) using superposition.

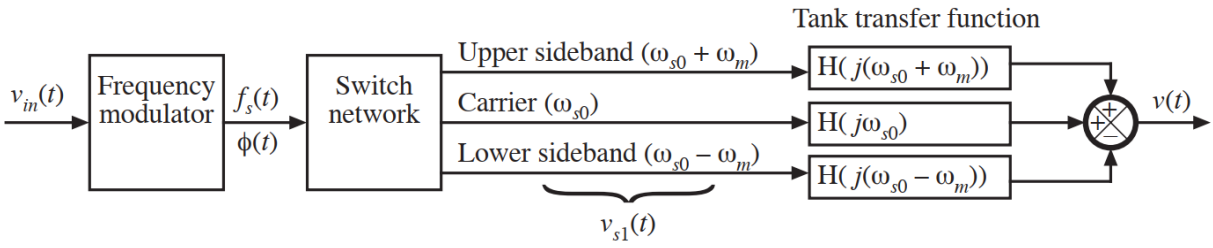

Figure 4.1: output voltage using superposition

Tank Transfer function is derived as:

$$H(s) = \frac{\frac{C_s L_p}{n} s^2}{1 + \frac{L_p}{R} s + (\frac{C_s L_p}{n^2} + L_s C_s + L_p C_p) s^2 + \frac{L_s C_s L_p}{R} s^3 + L_s L_p C_s C_p s^4}$$

Bode Plot for Transfer Function H(s) is shown in [Figure 4.2]

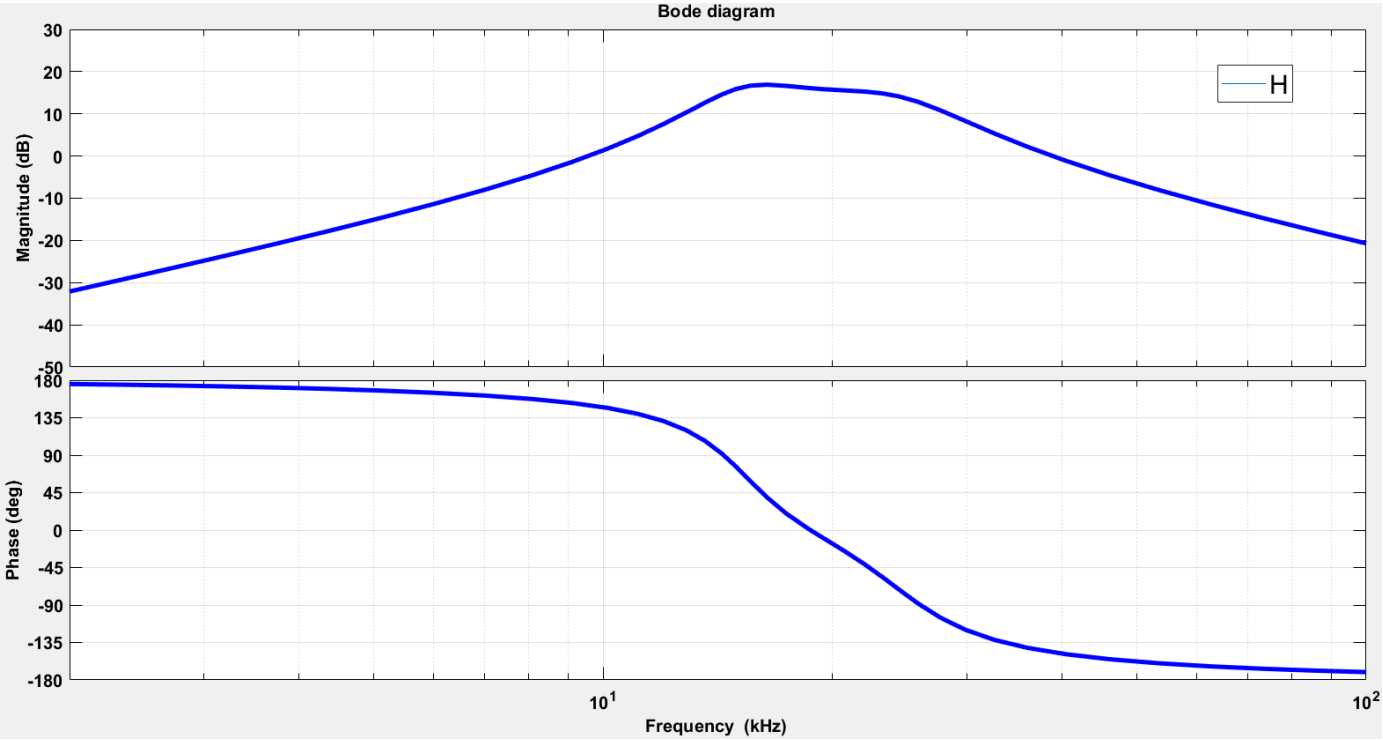

Figure 4.2: Magnitude and Phase of H(s)

A Matlab program is used for getting bode plots of small signal transfer functions. All three voltage envelop, current envelop and power envelop are obtained using that program.

4.2 LCLC Small-Signal Modeling

The direct modeling approach models the resonant inverter without transforming the resonant tanks or signals in the circuit to construct the equivalent circuits or state space equations. Instead it decomposes the modulated input to obtain its fundamental component as well as dominant sidebands. Superposition is then applied to get the total response to the modulated input.

In general, a modulated sinusoid can be expressed as the sum of a series of signals with frequencies Fs, Fs + fm, Fs - fm, Fs + 2fm, Fs - 2fm, etc. where Fs is the carrier frequency (for a switching power converter, it is the switching frequency) and fm is the modulating frequency or perturbing frequency. If the magnitude of the modulating signal is very small compared to the carrier signal (narrow-band modulation for FM, the modulated input can be simplified as the sum o f three dominant components with frequencies Fs, Fs + fm, Fs — fm where the magnitude of the fundamental component at Fs is much larger than the two sidebands. Based on above assumption, we can decompose the modulated input into three individual inputs as shown below. The input ac v_{in} to the resonant tank network based on sinusoidal approximation is

$$v_{in} = \frac{4}{\pi} V_{dc} \sin(\frac{\pi d(t)}{2}) \cos(w_s t)$$

where V_{dc} is dc bus voltage, d is the phase shift command (duty cycle). Introducing small perturbation in phase shift as

$$d(t) = D + \Delta d \cos(w_m t)$$

where D is the steady state duty cycle and Δd is the amplitude of perturbation and w_m is the perturbation frequency,

$$d(t) = D + \tilde{d}(t)$$

where

$$\tilde{d}(t) << D$$

$$v_{in} = \frac{4}{\pi} V_{dc} \sin(\frac{\pi(D + \tilde{d}(t))}{2}) \cos(w_s t)$$

Using trigonometric identities and simplification we can get,

$$v_{in} = \frac{4}{\pi} V_{dc} \sin(\frac{\pi D}{2}) \cos(w_s t) + \frac{4}{\pi} V_{dc} \cos(\frac{\pi D}{2}) \frac{\pi \tilde{d}(t)}{2} \cos(w_s t)$$

$$\tilde{d}(t) = \Delta d \cos(w_m t)$$

Using trigonometric identities, we can get the final expression for input voltage as:

$$v_{in} = \frac{4}{\pi} V_{dc} \sin(\frac{\pi D}{2}) \cos(w_s t) + V_{dc} \Delta d \cos(\frac{\pi D}{2}) [\cos((w_s - w_m)t) + \cos((w_s + w_m)t)]$$

The above expression shows the decomposed phase shift modulated input as three individual inputs with frequencies, Fs, Fs - fm, Fs+ fm.

4.2.1 Derivation

For easy derivation, we are defining some constants,

$$K_1 = \frac{4}{\pi} V_{dc} \sin(\frac{\pi D}{2})$$

$$K_2 = V_{dc} \Delta d \cos(\frac{\pi D}{2})$$

Now the Fourier transform of phase modulated input can be written as:

$$V_{in-PM}(jw) = K_1\pi[\delta(w - w_s) + \delta(w + w_s)] + K_2\pi[\delta(w - (w_s + w_m)) + \delta(w + (w_s + w_m))]$$
$$+ K_2\pi[\delta(w - (w_s - w_m)) + \delta(w + (w_s - w_m))]$$

The system response in frequency domain can be written as:

$$V_{out}(jw) = V_{in-PM}(jw)H(jw)$$
$$H(jw) = \frac{\frac{C_sL_p}{n}(jw)^2}{1 + \frac{L_p}{R}(jw) + (\frac{C_sL_p}{n^2} + L_sC_s + L_pC_p)(jw)^2 + \frac{L_sC_sL_p}{R}(jw)^3 + L_sL_pC_sC_p(jw)^4}$$

where $H(jw)$ is transfer function of LCLC resonant tank. Using above two equations and applying the identity $H(w)\delta(w - w_o) = H(w_o)\delta(w - w_o)$, we can express V_{out} as:

$$V_{out}(jw) = K_1\pi[H(jw_s)\delta(w - w_s) + H(-jw_s)\delta(w + w_s)]$$
$$+ K_2\pi[H(j(w_s + w_m))\delta(w - (w_s + w_m)) + H(-j(w_s + w_m))\delta(w + (w_s + w_m)]$$
$$+ K_2\pi[H(j(w_s - w_m))\delta(w - (w_s - w_m)) + H(-j(w_s - w_m))\delta(w + (w_s - w_m))]$$

Taking inverse Fourier transformation of $V_{out}(jw)$ we can obtain,

$$v_{out}(t) = \frac{1}{2}Ae^{jw_st} + \frac{1}{2}A^*e^{-jw_st}$$

$$v_{out}(t) = ||A|| \cos(w_st + \angle A)$$

The above equation represents a sinusoid having time varying amplitude or envelope and also a time varying phase, where $||A||$ and $\angle A$ are magnitude and phase of A respectively, and

$$A = A_o + A_ue^{jw_mt} + A_le^{-jw_mt}$$

$$A_o = K_1 H(jw_s)$$

$$A_u = K_2 H(j(w_s + w_m))$$

$$A_l = K_2 H(j(w_s - w_m))$$

$$V_{out-en} = ||A||$$

where V_{out-en} represents the envelope of $V_{out}(t)$. Now we need to process the envelope and extract the small signal transfer function. As we know

$$\begin{aligned} ||A||^{\,2} = AA^* &= (A_o + A_u e^{jw_m t} + A_l e^{-jw_m t})(A_o^* + A_u^* e^{-jw_m t} + A_l^* e^{jw_m t}) \\ &= ||A_o||^{\,2} + ||A_u||^{\,2} + ||A_l||^{\,2} \\ &\quad + 2||A_o A_l^* + A_o^* A_u||\ \cos(w_m t + \angle(A_o A_l^* + A_o^* A_u)) \\ &\quad + 2||A_l^* A_u||\ \cos(2w_m t + \angle(A_l^* A_u)) \end{aligned}$$

For small variations in phase shift command, we apply the small signal assumption as $||A_u||\ , ||A_u|| \ << ||A_o||$ to neglect $||A_u||^{\,2}$ and $||A_u||^{\,2}$ as well as component with $2w_m$, which gives,

$$||A||^{\,2} = ||A_o||^{\,2} + 2||A_o A_l^* + A_o^* A_u||\ \cos(w_m t + \angle(A_o A_l^* + A_o^* A_u))$$

Above equation expresses $||A||^{\,2}$ as sum of steady state portion and small signal portion. The small signal portion gives the variation of output power in response to the phase shift perturbation. Output power can be obtained as:

$$p_{out-en} = \frac{||v_{out}||^2}{2R} = \frac{||A||^2}{2R}$$

$$p_{out-en} = \frac{||A_o||^{\,2}}{2R} + \frac{||A_o A_l^* + A_o^* A_u||}{R} \cos(w_m t + \angle(A_o A_l^* + A_o^* A_u))$$

As we have set initial phase of phase modulation sinusoid to zero and magnitude to Δd , the magnitude and phase of the ac component correspond to the magnitude and phase of small signal transfer function from phase shift command to output power envelope, respectively. By defining,

$$p_{out-en} = P_{out-en} + \hat{p}_{out-en}$$

$$d = D + \hat{d}$$

$$G_{p_{env}} = \frac{\hat{p}_{out-en}}{\hat{d}}$$

we can obtain,

$$||G_{p_{env}}(jw_m)|| = \frac{1}{\Delta d}\frac{||A_o A_l^* + A_o^* A_u||}{R}$$

$$\angle G_{p_{env}}(jw_m) = \angle(A_o A_l^* + A_o^* A_u)$$

Combining the magnitude and phase expression, we can obtain the transfer function from phase shift command to output power envelope as:

$$G_{p_{env}}(jw_m) = \frac{1}{\Delta d}\frac{A_o A_l^* + A_o^* A_u}{R}$$

where A_o , A_l and A_u are already defined in previous equations. By replacing jw_m with s and substituting values of A_o , A_l and A_u in above equation we can get the transfer function in s domain as:

$$G_{p_{env}}(s) = \frac{K_1 K_2}{\Delta d R}[H(jw_s)H(s - jw_s) + H(-jw_s)H(s + jw_s)]$$

This method can be extended to find the transfer functions for voltage and current envelope to the phase shift command. As we know from the previous equation,

$$||A||^{\,2} = ||A_o||^{\,2} + 2||A_o A_l^* + A_o^* A_u||\ \cos(w_m t + \angle(A_o A_l^* + A_o^* A_u))$$

By taking square root of $||A||^{\,2}$, we obtain

$$||A|| = \sqrt{||A_o||^{\,2} + 2||A_o A_l^* + A_o^* A_u|| \cos(w_m t + \angle(A_o A_l^* + A_o^* A_u))}$$

Using linearization and small signal assumption, we can obtain

$$v_{out-en} = ||A_o|| + \frac{||A_o A_l^* + A_o^* A_u||}{||A_o||} \cos(w_m t + \angle(A_o A_l^* + A_o^* A_u))$$

Above equation contains dc component and ac component, by defining

$$v_{out-en} = V_{out-en} + \hat{v}_{out-en}$$

$$d = D + \hat{d}$$

$$G_{v_{env}} = \frac{\hat{v}_{out-en}}{\hat{d}}$$

we can obtain,

$$||G_{v_{env}}(jw_m)|| = \frac{1}{\Delta d} \frac{||A_o A_l^* + A_o^* A_u||}{||A_o||}$$

$$\angle G_{v_{env}}(jw_m) = \angle(A_o A_l^* + A_o^* A_u)$$

Similar to above method, we can obtain transfer function of phase shift to output voltage in s domain by replacing jw_m with s as:

$$G_{v_{env}}(s) = \frac{K_2}{\Delta d||H(jw_s)||}[H(jw_s)H(s - jw_s) + H(-jw_s)H(s + jw_s)]$$

Similarly we can find phase shift to current envelope transfer function in s domain as

$$G_{i_{env}}(s) = \frac{K_2}{\Delta d||H(jw_s)||R}[H(jw_s)H(s - jw_s) + H(-jw_s)H(s + jw_s)]$$

Given the LCLC parameters from Table 3.3, the magnitude and phase responses of the output power, voltage, and current envelope transfer functions are shown in Figure 4.3 for the

load R = 1100 ohm and D = 0.9. A MATLAB program for obtaining phase shift command to output power transfer functions is used. MATLAB program is given in Appendix A.

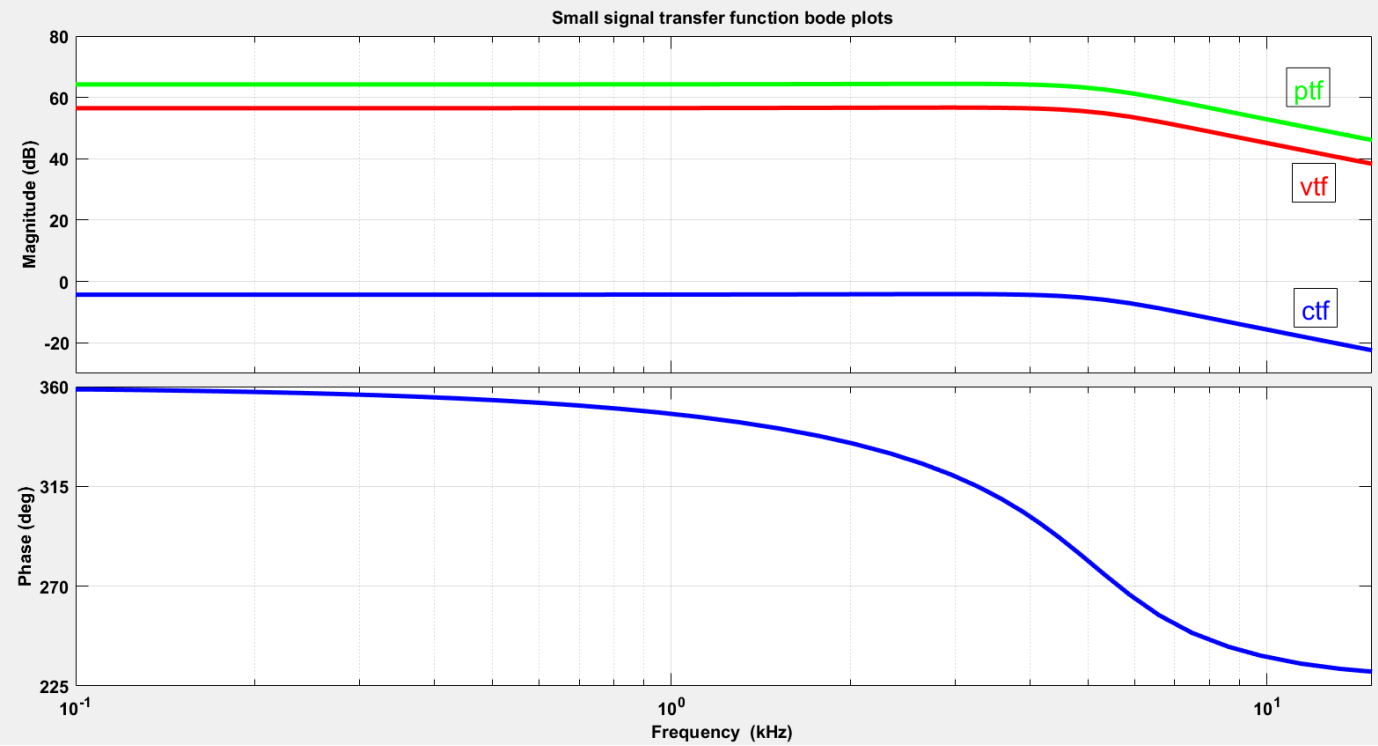

Figure 4.3: Transfer functions for Vin = 350 V , D = 0.9, and R = 1100 Ω: power (green), voltage (red), and current (blue).

4.3 Control Techniques

Control of active power delivered to the load is a major issue in building a ultrasonic generator for welding system. For covering a wide range of output power, two control techniques are proposed in the literature [9].

1. Duty Control

2. Frequency Control

For this purpose there are two PWM signals out of phase with each other by 180^{0} should be generated. For low power levels from 0 to about 20% of nominal power of the generator, algorithm is based on duty cycle control. It is used mainly during the beginning and end of weld cycle when the power isn't too high or when the weld area is small. Above 20% of the nominal power of the generator the control algorithm maintains the duty cycle of both signals at 50% and changes their frequency according to the needed power level. The working range is between series resonance frequency and parallel resonance frequency. The algorithm always starts from the higher frequency, which is the parallel resonance frequency and works downward until the desired or maximum output power level is reached.

In ultrasonic welding active power level is a function of three parameters. First two are the amplitude of voltage on and current flowing through piezoelectric transducer. Third one is the frequency of electric signal which powers the converter. In order to obtain sufficient accuracy of power stabilization ultrasonic generator must be capable of retuning these parameters by small extent and within very short period of time. This is most important in case of frequency control because even a shift of 0.1 Hz can have a significant effect on power output of ultrasonic stack. Also while keeping the 0.1 Hz accuracy the generator must be able to change the frequency in the range of 1 kHz above and below the nominal frequency.

One of the approach of digital control is proposed in literature[10]. In this approach the voltage and current are measured using ADCs, and the resulting digital values are input to the digital controller. Both voltage and current measurements are necessary for maintaining

constant power output. The control technique devised for the prototype samples the output voltage and current 15 times per switching period, then averages the resulting product.

4.4 PI compensator design

We have found out the small signal phase shift command to output power transfer function in previous section. To design a compensator we have used the bode plots of transfer function obtained from Matlab program. The dc gain values is 63.2 dB taken from bode plot (D = 0.9) and also the crossover frequency is assumed as 5 kHz. Therefore the compensator should have -63.2 dB gain at crossover frequency. Phase margin is assumed to be 60 degrees. Compensator should provide the required phase for this system. The transfer function phase at 5 kHz is -78 degrees.

The PI compensator is given by,

$$G_c(s) = P + \frac{K_i}{s}$$

To get the 60 degree phase margin, the compensator should have -42 degrees phase at crossover frequency,

$$G_c(s) = \frac{sP + K_i}{s}$$

$$G_c(jw) = \frac{jwP + K_i}{jw}$$

$$tan^{-1}(\frac{w_c P}{K_i}) - 90 = -42$$

$$\frac{w_c P}{K_i} = 1.1106$$

$$\frac{K_i}{w_c}\sqrt{1 + (\frac{w_c P}{K_i})^2} = 0.0006918$$

From above equations, we are able to get values of P and K_i as $P = 0.00051415$ $K_i = 14.544$

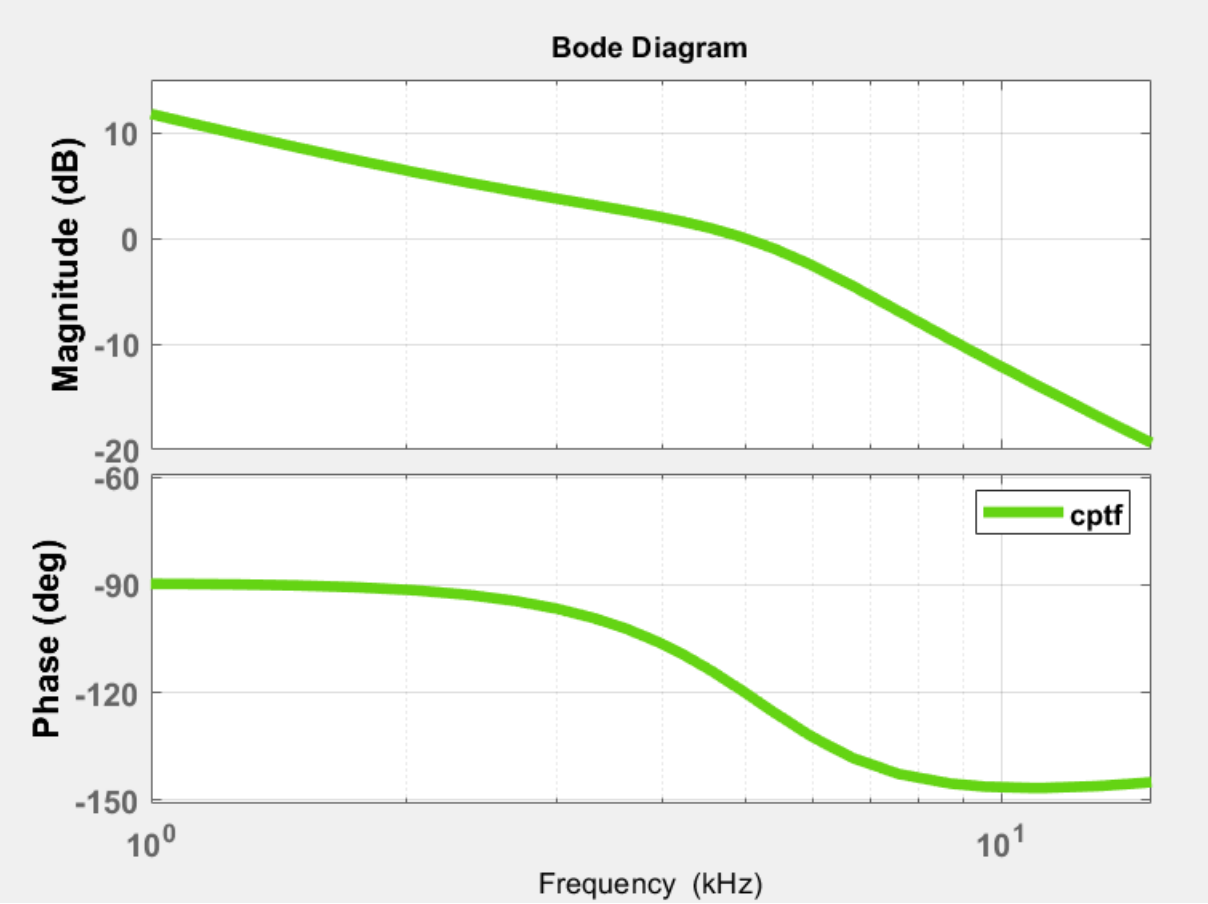

Figure 4.4: Compensated loop gain bode for D=0.9,R1= 1100 ohm

4.5 Closed loop control model

For closed loop control model, we have done simulations in PLECS software. Active power is given as feedback and compared with reference power curve . Using above compensator design, control system is able to track the reference power. Active power is calculated by rms

load rms current and is given as feedback. The error signal is then go through compensator and phase shift block to generate phase shifted pulses for full bridge Mosfet switches. Output power tracking graph is shown in Figure 4.6. Bridge output voltage and current are shown in Figure 4.7.

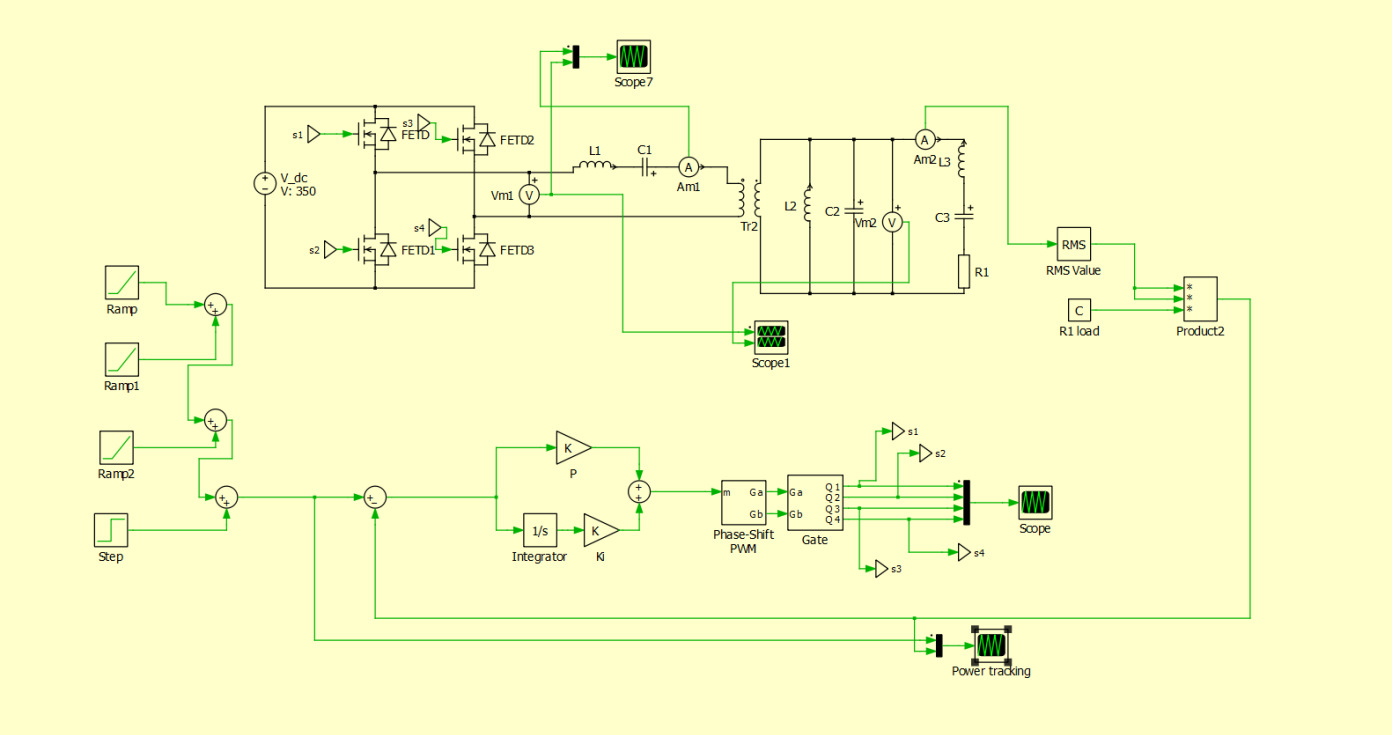

Figure 4.5: Closed loop control model

Figure 4.6: Output power curve with reference tracking

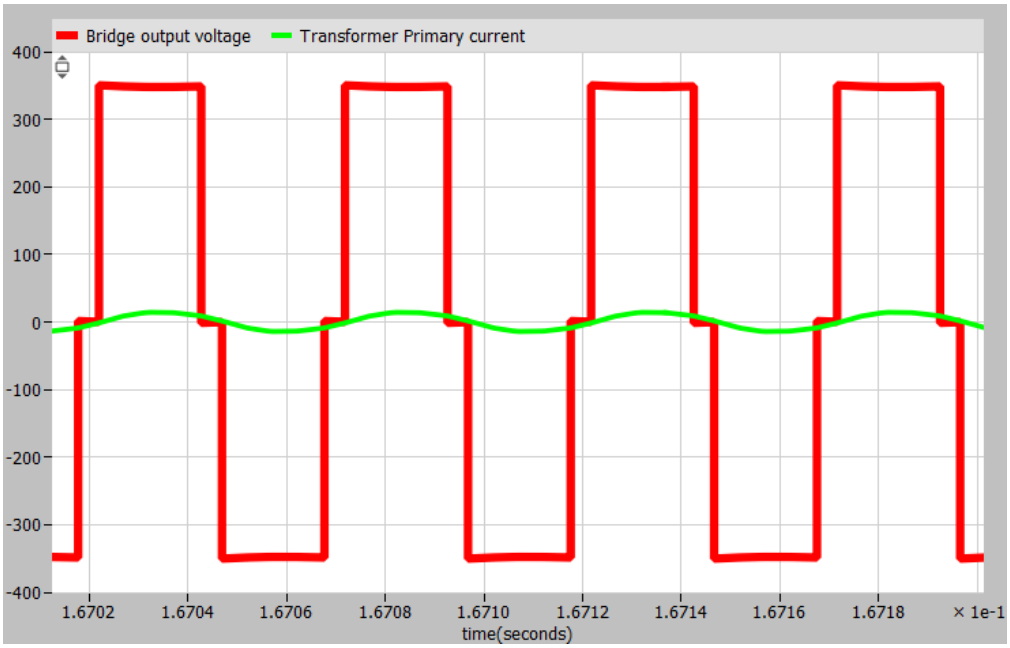

Figure 4.7: Bridge output voltage and current

Chapter 5

Conclusion and Future work

Ultrasonic welding is very useful and new technology. The same technology is used in various other applications such as drilling, cutting and cleaning. Ultrasonic welding is very fast and efficient way of welding. We have done detailed study about Ultrasonic transducers and their applications in industries. Ultrasonic transducers have certain impedance characteristics containing two resonant frequencies. Most of the time ultrasonic transducers are designed to work in range of these frequencies to get the maximum power output. As a part of the project we have developed a model for 3 kW ultrasonic welding generator. In chapter 1 of this work, we have given an introduction of the ultrasonic welding technology and its components and their uses.

Chapter 2 discusses the modeling of piezoelectric converter models and impedance characteristics of the ultrasonic transducers. Inductive compensation is done for the dielectric capacitance of the piezoceramic rings of ultrasonic transducer. Usage of resonant converter is discussed for this particular application. LLCC resonant converter is studied and simulated

in MATLAB. Full bridge topology is used. Phase shift between the two legs of full bridge is used to get the desired voltage at the bridge output.

Design of tank parameter values is carried out in chapter 3. Short circuit and open circuit impedance analysis is done for achieving zvs for a range of loads in frequency ranges. Inductance and capacitance ratio is varied to get the desired THD values for the output voltage and currents.

Modeling of converter is done by using envelope method and small signal transfer functions are obtained. Envelope modeling is simple and easy technique because of usage of tank transfer function H(S) directly in analysis. Phase shift is used as control parameter for this model. Different control techniques are discussed in chapter 4. PI compensator design is carried out and closed loop control model is simulated in PLECS software. Active power is following the desired output power reference. Results are shown for simulations done in this work.

Future work

1. Hybrid control scheme implementing both frequency control and duty control.
2. Efficiency and power loss calculations.
3. Resonant frequency tracking algorithms for ultrasonic transducers.

Chapter 6

References

[1] W. Kardyś, A. Milewski, P. Kogut, P. Kluk, Universal ultrasonic generator for welding, Acta Physica Polonica A, Vol. 124, No. 3, pp. 456-458, 2013

[2] M. Prokic, Piezoelectric Transducers Modeling and Characterization, MPI, Switzerland, 2004

[3] J. Chudorliński, W. Kardyś Usage of resonant converters in ultrasonic generators, Elektronika, Vol. 51, No. 7, pp. 99-102, 2010 (in Polish)

[4] C. Kauczor, T. Schulte, and N. Fröhleke. Resonant power converter for ultrasonic piezoelectric converter. Proceedings of 8th International Conference on New Actuators, ACTUATOR 2002, Bremen, 2002.

[5] Yong-Ann Ang, Modelling, Analysis and Design of LCLC Resonant Power Converters thesis.

[6] Erickson, R. W.; Maksimovic, D.: Fundamentals of Power Electronics, Second Edition, Kluwer Academic Publishers, Norwell-Massachusetts, 2001

[7] Rongyuan Li, Power Supplies for High-Power Piezoelectric Multi-Mass Ultrasonic Motor Diss. EIM-E/263

[8] Y. Yin, R. Zane, R. Erickson, and J. Glaser, Direct modeling of envelope dynamics in resonant inverters," Electronics Letters, vol. 40, pp. 834-836, 2004

[9] Brylski M. (2010b), Follow-up power adjustment in ultrasonic assembly of ultrasonic welding system [in Polish], Elektronika, 51, 7, 105–107.

[10] Jensen, S. "Fast Tracking Current Driven Electrosurgical Generator." (2015).

Appendix A

Matlab program

```
%program for small signal transfer function using direct envelope modeling

%start of program

global H;   % Resonant-tank transfer function v/vs1

global fs;  % Swithcing frequency [Hz]


Vg = 350;       % input voltage

Vs1 = 4*Vg/pi; % amplitude of the fundamental voltage at the input of the resonant tank

fs = 20.053e3; % steady-state switching frequency fs

D = 0.9;        % phase shift command (duty)


% define resonant tank transfer function

% change definition of H(s) to get Genv for other resonant tanks
```

```
s = tf('s');

R = 1100;

Lp = 6.848e-3;

Cp = 9.2e-9;

n = 6.37;

Ls = (20.544e-3)/(n^2);

Cs = (3.527e-9)*(n^2);


H =(((Cs*Lp)/(n))*(s^2))/(1 + (Lp/R)*(s) +

(s^2)*(((Cs*Lp)/(n^2))+Ls*Cs+Lp*Cp)+

(s^3)*((Ls*Cs*Lp)/R)+(s^4)*(Ls*Lp*Cs*Cp));

% series - parallel resonant inverter


%%calculation of transfer functions


K1 = Vs1*sin((pi*D)/2);

K2 = Vg*cos((pi*D)/2);

a  = Ls*Lp*Cs*Cp ;

b  = (Ls*Cs*Lp)/R ;

c  = ((Cs*Lp)/(n^2))+Ls*Cs+Lp*Cp ;

d  =  Lp/R ;

e  =  (Cs*Lp)/n ;

w_so = 2*pi*fs ;


H_jwso = tf([e*(1i*w_so)^2],[a*(1i*w_so)^4+b*(1i*w_so)^3+c*(1i*w_so)^2+d*(1i*w_so)+1]) ;

H_jwso_conj = tf([e*(-1i*w_so)^2],[a*(-1i*w_so)^4+b*(-1i*w_so)^3
```

```
                +c*(-1i*w_so)^2+d*(-1i*w_so)+1]) ;


s = 1i*w_so ;
H1 = evalfr(H,s);
H2 = abs(H1);


H_jwsopluswm = tf([e 1i*2*e*w_so e*(1i*w_so)^2 ],[a (4*a*1i*w_so+b)
                  (6*a*(1i*w_so)^2+3*b*(1i*w_so)+c)
                  (4*a*(1i*w_so)^3+
                  3*b*(1i*w_so)^2+2*c*(1i*w_so)+d) (a*(1i*w_so)^4+
                  b*(1i*w_so)^3+c*(1i*w_so)^2+d*(1i*w_so)+1)]);
                  H_jwsominuswm_conj = tf([e -1i*2*e*w_so e*(-1i*w_so)^2 ],
                  [a (4*a*(-1i*w_so)+b) (6*a*(-1i*w_so)^2+3*b*(-1i*w_so)+c)
                  (4*a*(-1i*w_so)^3+3*b*(-1i*w_so)^2+2*c*(-1i*w_so)+d)
                  (a*(-1i*w_so)^4+b*(-1i*w_so)^3+c*(-1i*w_so)^2+d*(-1i*w_so)+1)]);


htf =   H_jwso*H_jwsominuswm_conj + H_jwso_conj*H_jwsopluswm;
ptf =  ((K1*K2)/R)*(H_jwso*H_jwsominuswm_conj + H_jwso_conj*H_jwsopluswm);
%power envelope small signal transfer function
vtf =  ((K2)/H2)*(H_jwso*H_jwsominuswm_conj + H_jwso_conj*H_jwsopluswm);
%voltage envelope small signal transfer function
ctf =  ((K2)/(H2*R))*(H_jwso*H_jwsominuswm_conj + H_jwso_conj*H_jwsopluswm);
%current envelope small signal transfer function


%bode plot for LCLC tank transfer function
```

```
figure(1)

fmin = 2;

fmax = 100;

BodeOptions = bodeoptions;

BodeOptions.FreqUnits = 'kHz';

BodeOptions.Xlim = [fmin fmax];

BodeOptions.Ylim = {[-50,30];[-180,180]};

BodeOptions.Grid = 'on' ;

bode(H,BodeOptions);

set(findall(gcf,'Type','line'),'LineWidth',3,'Color','blue')

%bode plots for small signal transfer functions

figure(2)

fmin1 = 0.1;

fmax1 = 15;

BodeOptions1 = bodeoptions;

BodeOptions1.FreqUnits = 'kHz';

BodeOptions1.Xlim = [fmin1 fmax1];

BodeOptions1.Ylim = {[-50,100];[-180,180]};

BodeOptions1.Grid = 'on' ;

bode(ptf,BodeOptions1);

set(findall(gcf,'Type','line'),'LineWidth',3,'color','green')

hold on;

BodeOptions2 = bodeoptions;

BodeOptions2.FreqUnits = 'kHz';

BodeOptions2.Xlim = [fmin1 fmax1];

BodeOptions2.Ylim = {[-50,100];[-200,200]};
```

```
BodeOptions2.Grid = 'on' ;

bode(vtf,BodeOptions2,'r');

set(findall(gcf,'Type','line'),'LineWidth',3)

hold on;

BodeOptions3 = bodeoptions;

BodeOptions3.FreqUnits = 'kHz';

BodeOptions3.Xlim = [fmin1 fmax1];

BodeOptions3.Ylim = {[-30,80];[-200,200]};

BodeOptions3.Grid = 'on' ;

bode(ctf,BodeOptions3,'b');

set(findall(gcf,'Type','line'),'LineWidth',3)

hold on;

hold off;

% compensated loop gain bode

picomp = tf([5.1415e-4 14.5439],[1 0]);  %pi compensator transfer function

cptf = ptf*picomp ;                      %compensated loop gain transfer function

bode(cptf);                              %compensated loop gain bode plot
```